

Kinematic Effects of Tidal Interaction on Galaxy Rotation Curves ¹

Elizabeth J. Barton

Harvard-Smithsonian Center for Astrophysics

and

Benjamin C. Bromley

Department of Physics, University of Utah

and

Margaret J. Geller

Harvard-Smithsonian Center for Astrophysics

ABSTRACT

We use self-consistent N-body models, in conjunction with models of test particles moving in galaxy potentials, to explore the initial effects of interactions on the rotation curves of spiral galaxies. Using nearly self-consistent disk/bulge/halo galaxy models (Kuijken & Dubinski 1995), we simulate the first pass of galaxies on nearly parabolic orbits; we vary orbit inclinations, galaxy halo masses and impact parameters. For each simulation, we mimic observed rotation curves of the model galaxies. Transient interaction-induced features of the curves include distinctly rising or falling profiles at large radii and pronounced bumps in the central regions. Remarkably similar features occur in our statistical sample of optical emission-line rotation curves of spiral galaxies in tight pairs and n-tuples.

Subject headings: galaxies: interactions — galaxies: kinematics and dynamics

1. Introduction

Observations of interacting pairs of galaxies in the nearby universe reveal a rich set of phenomena, including starbursts, tidal tails, streams, bridges and shells, which arise as companions perturb or even disrupt the galaxies (see Barnes & Hernquist 1992; Sanders & Mirabel 1996). These features, if unique to interacting systems, may offer probes of the extent of dark halos in individual galaxies, the rate of galaxy mergers, and the evolution of galactic structure. Thus,

¹Some observations reported in this paper were obtained at the Multiple Mirror Telescope Observatory, a facility operated jointly by the University of Arizona and the Smithsonian Institution.

analysis of interacting galaxies may provide strong constraints for cosmological models: the mass in dark halos may be the single most important contribution to the cosmological mass density parameter Ω . The galaxy merger rate is also sensitive to the form of the primordial power spectrum and hence the nature of dark matter.

Complete samples of interacting galaxies are valuable for understanding the range of dynamical processes which are important in galaxy evolution, and for the constraints they can place on the *average* halo mass fraction and merger rates. Members of a late-stage merger may be unresolved, making morphological selection of complete samples difficult. Nonetheless, merging pairs identified by morphology or infrared emission can yield interesting results (e.g. the halo mass constraints: Dubinski, Mihos, & Hernquist 1996; Hibbard & Mihos 1995; Springel & White 1998; ULIGs: see Sanders & Mirabel 1996 for a review).

The early stages of interaction are easier to survey and to study statistically because the systems are resolvable galaxy pairs. Galaxy pair studies employ a variety of selection criteria (e.g. Vorontsov-Vel'yaminov 1959; Arp 1966; Karachentsev 1972, 1987; Turner 1976a, 1976b; Chengalur, Salpeter, & Terzian 1993, 1994, 1996) and selection effects may be difficult to model. A few authors have attempted statistical studies of the rotation curves of interacting galaxies (Chengalur *et al.* 1994; Keel 1993, 1996; Márquez & Moles 1996).

Complete redshift surveys allow detailed control of all selection effects of complete pair samples. In observation times that permit construction of large samples, rotation curves provide kinematic data over a strip of each galaxy. Barton *et al.* (1998b) measured ~ 140 emission line rotation curves in pairs selected from the CfA2 redshift survey (Geller & Huchra 1989; Huchra, Vogeley, & Geller 1998; Falco *et al.* 1998). The data display features which are consistent with Keel's (1993;1996) qualitative studies of rotation curves in a sample of paired and interacting galaxies.

This Letter is an investigation of the signatures of interaction in galaxy pairs during the early stages of interaction or merging. Our numerical work with dissipationless N-body simulations (Barton *et al.* 1998a) illustrates that rotation curves of spiral galaxies in pairs can bear specific, predictable signatures of interaction: the flat rotation curves typically associated with these objects in isolation acquire distinct features such as dips near the galactic nucleus and sharply rising or falling profiles in the outer regions of the galactic disk. These features can reflect non-circular motion and depend on the internal structure of the individual galaxies and the orbital parameters of the interaction.

2. Numerical Method

The first step toward simulating galaxy pair interactions is to construct model galaxies with disk, bulge and halo components. We follow the general prescription of Kuijken & Dubinski (1995), correcting a sign error in their equation 2. The method generates near-equilibrium phase-space

distributions of galaxies in isolation. For the purposes of this study we select three models which reproduce the Galactic rotation curve out to roughly 5 disk scale lengths. These models, labeled Milky Way (MW) A, B, and D by Kuijken & Dubinski, have halo-to-(disk+bulge) mass ratios of 4:1, 8:1 and 30:1, respectively, and radial extents of 22, 30, and 73 in units of the characteristic disk scale length. For the Milky Way, the length unit in the models has an approximate physical value of 4.5 kpc, while the time and velocity units discussed below correspond to 20 Myr and 220 km/s, respectively.

We generate realizations of the Kuijken–Dubinski MW models with discrete particles and evolve them, both in isolation and in pairs, using a gravity treecode (Barnes & Hut 1986; Hernquist 1987). In the simulations, individual galaxies consist of 50,000 or 100,000 particles; the treecode’s particle-cell force calculations are performed with opening angle $\theta \leq 0.7$, monopole cell-mass approximations, and a Plummer smoothing parameter of $\epsilon = 0.05$. The integrator is a leapfrog algorithm with a timestep of $\Delta t = 0.01$ units.

To improve our ability to trace the behavior of the outer disk accurately, we also consider galaxy pair models which consist of the analytical Kuijken–Dubinski potentials moving along trajectories determined from the self-consistent N -body simulations. We track the kinematical evolution of the disk components with test particles (see Dubinski, Hernquist, & Mihos 1997). Thus, at little computational expense we can model well-resolved disks with $N = 100,000$ particles and without the effects of discreteness such as artificial disk heating by massive halo particles.

A comparison between the self-consistent N -body simulations and the kinematical models demonstrates that the bulk flows of disk material, and hence rotation curves, are qualitatively similar. Even detailed, quantitative differences are negligible unless the halo mass is relatively high (as in the MW D models) or unless the impact parameter of the mass centers is less than 2 units (as measured from the initial parabolic orbits). Thus we justify our ample use here of the kinematical models and their more highly resolved rotation curves.

We start the galaxies on initially parabolic orbits ($E_0 = 0$) which eventually lead to mergers due to dynamical friction. The galaxies start with dark matter halos touching (except the large Milky Way D model), following Dubinski *et al.* (1997). We observe no significant disturbance in the disk and bulge particles in the early timesteps, until about $T \gtrsim 30$, indicating that results are insensitive to the proximity of the galaxies at startup.

3. Results

Figs. 1 illustrates some of the most dramatic kinematic effects shortly after the first pass. The figure shows positions and velocities of particles from the kinematic simulations with various inclinations, model halo sizes and impact parameters. We plot the galaxies and rotation curves at ~ 5 –8 time units after closest approach, when the kinematic response is dramatic. We rotate some galaxies in their disks’ planes to compare responses. The figure caption gives the starting galaxy

parameters and Toomre disk orientation parameters i and ω (Toomre & Toomre 1972). For ω , we quote the argument of periaapse, using bulge centers for the galaxy positions; b is the bulge separation at closest approach.

The galactic disks, and the orbits of the fully prograde and retrograde galaxies, are in the x-y plane, the plane of the paper in the upper half of each square. In the lower half of each square, we show the velocities as if we were observing the galaxy inclined only 5° from edge-on, at a distance of 77 Mpc through a 1.5 arcsecond slit. Thus, x-positions of the particles are plotted vs. (nearly) y-velocities. We incline the galaxy by this small amount in order to mimic longslit observations of velocities near the the projected disk major axis. In Fig. 1, the solid line is the rotation curve we derive from the simulation to compare with measured optical rotation curves of galaxies. To compute this curve, we smear each particle in the x-direction by a “seeing function”, a Gaussian of 1 arcsecond (assuming a distance of 77 Mpc). We then find the “flux”-weighted velocity mean at various positions along the slit.

During the simulations, non-circular motions result as the outer disk is tidally ripped into tails. As the orbital pass progresses, the outer portions of the curve, initially flat, are stretched into rising, falling, or bent lines. The rotation curve for the same galaxy at the same time can rise or fall, depending on the viewing angle. The inner disk distorts into a bar-like, elongated structure which has almost no effect on the center of the rotation curve, the solid-body portion. For a period of time after the first pass of strong enough interactions, the inner and outer portions of the galaxy appear as distinct kinematic components — a lump on the inside and a distorted outer region. This kinematic pattern resembles the two-component kinematic structure associated with both bars and circumnuclear gas disks (Rubin, Kenney, & Young 1997). The pattern does not require dissipative matter to form — it can form without gas infall. At later times, the tails become sparse as they begin to settle back onto the galaxy.

Encounters with smaller impact parameters appear to produce narrower, more well-defined central bumps, as well as richer and sometimes longer tidal tails with more dramatic kinematic features. Not surprisingly, prograde encounters give rise to the most dramatic responses — the longest tidal tails and the most kinematic tidal ripping. Retrograde encounters show almost no response. As Dubinski *et al.* (1996) note, tail formation is suppressed in collisions of Milky Way D models. We can measure the true differences among the models by “observing” the simulations at a large number of random orientations for comparison with a complete observational sample.

4. Discussion

A range of observational phenomena in our statistical sample of optical rotation curves of galaxies in pairs (Barton *et al.* 1998b) may reflect interactions like those simulated in Fig. 1. Fig. 2 shows striking examples of galaxies with interesting kinematics. In each B image, the arrow shows the position of the spectrograph slit; the arrow points in the direction of increasing position

on the rotation curve plot. The curves are centered — the zero position is approximately the flux center of the continuum. Fig. 2a shows NGC 4676, or “The Mice”. The northern galaxy, shown to the right in our image, has one of the most dramatic tidal tails in our pair sample; the rotation curve clearly shows the rising pattern. Fig. 2b shows UGC 484, a paired barred spiral 46 h^{-1} projected kpc from a companion galaxy. Its rotation curve displays the multi-component kinematic structure which may be associated with the bar. The inner region shows a steep rise; the slower nearly solid-body rotation in the middle region extends for $\sim 12 \text{ h}^{-1}$ projected kpc before the curve flattens.

The pair sample (Barton *et al.* 1998b), consists of ~ 140 spiral and S0 galaxies in spiral/spiral and spiral/elliptical pairs that are appropriate for longslit emission observations. This “dynamical” sample, when properly compared with control samples and simulations, will enable estimation of the frequency of interaction-induced features. Although we observe < 5 disk scale lengths, we find some curves which rise or, less frequently, fall; some of these curves eventually flatten. We also find some dips in the center which may be associated with circumnuclear bars or gas disks (Rubin *et al.* 1997). Curves of the most distorted galaxies appear bumpy and irregular. These phenomena are similar to effects noted by Keel (1993, 1996).

A compelling argument linking particular features in rotation curves to interactions is difficult. Statistical observational studies can link rotation curve features to known interaction phenomena (Keel 1993). Simulations and models can show the physical basis for interaction features (e.g. tails, bridges, kinematic features: Toomre & Toomre 1972; Byrd 1976; Borne 1988a, 1988b; Byrd & Klaric 1990; Elmegreen *et al.* 1995a, 1995b; Combes *et al.* 1995; Dubinski *et al.* 1996; gas infall: Negroponte & White 1983; Noguchi 1991). We extend this work with systematic simulations and exploration of features that might appear in a large sample of rotation curves of galaxies in interacting pairs. However, there are many aspects of galaxy interactions and rotation curve measurement we do not model, including: (1) instrumental effects such as slit misalignment, (2) gas-related phenomena such as gas infall and star formation (e.g. Barnes & Hernquist 1992; Mihos & Hernquist 1996) (3) lumpy, non-uniform emission and dust which affect rotation curve measurement, (4) varied starting galaxy potentials including halos with significant angular momentum and massive halos with shallow potentials, and (5) environmental effects such as background potentials.

We will present a more detailed description of these simulations (Barton *et al.* 1998a) as well as the data (Barton *et al.* 1998b). We plan to enlarge our simulation study to explore a greater portion of parameter space; we will study the frequency and duration of interaction-induced kinematic features, as well as their dependence on orbital inclination and energy (including collisions that do not result in mergers) and starting model parameters.

Our principle result is that we reproduce some of the interesting features seen in the rotation curves of galaxies in our sample. These features in our simulated rotation curves are associated with tidal shearing and subsequent infall. Even without gas in our simulations, we produce

two-component kinematic structures similar to dips in observed rotation curves associated with both bars and circumnuclear gas disks (Rubin *et al.* 1997).

During interactions, rotation curves derived from line-of-sight velocity measurements deviate from circular speed curves. Thus, our simulations illustrate the danger of inferring galaxy potentials from observed kinematics when interactions may be a factor.

We thank Antonaldo Diaferio, Mike Kurtz and Lars Hernquist for very useful discussions and aid. EJB received support from a Harvard Merit Fellowship. BCB acknowledges funding from NSF Grant PHY 95-07695. We are grateful to the Caltech Center for Advanced Computing Research and NASA Offices of Space Sciences, Aeronautics, and Mission to Planet Earth for providing computing resources.

REFERENCES

- Arp, H. 1966, *ApJS*, 14, 1
- Barnes, J. E., & Hernquist, L. 1992, *ARA&A*, 30, 705
- Barnes, J. E., & Hut, P. 1986, *Nature*, 324, 446
- Barton, E. J., *et al.* 1998a, in preparation
- Barton, E. J., *et al.* 1998b, in preparation
- Borne, K. D. 1988a, *ApJ*, 330, 38
- Borne, K. D. 1988b, *ApJ*, 330, 61
- Byrd, G. G. 1976, *ApJ*, 208, 688
- Byrd, G. G., & Klaric, M. 1990, *AJ*, 99, 1461
- Chengalur, J. N., Salpeter, E. E., & Terzian, Y. 1993, *ApJ*, 419, 30
- Chengalur, J. N., Salpeter, E. E., & Terzian, Y. 1994, *AJ*, 107, 1984
- Chengalur, J. N., Salpeter, E. E., & Terzian, Y. 1996, *ApJ*, 461, 546
- Combes, F., Rampazzo, R., Bonfanti, P. P., Pringniel, P., & Sulentic, J. W. 1995, *A&A*, 297, 37
- Dubinski, J., Mihos, J. C., & Hernquist, L. 1996, *ApJ*, 462, 576
- Dubinski, J., Hernquist, L., & Mihos, J. C. 1997, preprint
- Elmegreen, D. M., Kaufman, M., Brinks, E., Elmegreen, B. G., & Sundin, M. 1995a, *ApJ*, 453, 100
- Elmegreen, B. G., Sundin, M., Kaufman, M., Brinks, E., & Elmegreen, D. M. 1995b, *ApJ*, 453, 139

- Falco, E. E., Kurtz, M. J., Geller, M. J., Huchra, J. P., Peters, J., Berlind, P., Tokarz, S., & Elwell, B. 1998, in preparation
- Geller, M. J., & Huchra, J. P. 1989, *Science*, 246, 897
- Hernquist, L. 1987, *ApJS*, 64, 715
- Hibbard, J. E., & Mihos, J. C. 1995, *AJ*, 110, 140
- Huchra, J. P., Vogeley, M. S., & Geller, M. J. 1998, submitted
- Karachentsev, I. D. 1972, *Soobsh. Spets. Astrof. Obs.*, 7, 3
- Karachentsev, I. D. 1987, *Dvoinye Galaktiki (Nauka: Moscow)*
- Keel, W. C. 1993, *AJ*, 106, 1771
- Keel, W. C. 1996, *ApJS*, 106, 27
- Kuijken, K., & Dubinski, J. 1995, *MNRAS*, 277, 1341
- Márquez, I., & Moles, M. 1996, *A&AS*, 120
- Mihos, J. C., & Hernquist, L. 1996, *ApJ*, 464, 641
- Negroponte, J., & White, S. D. M. 1983, *MNRAS*, 205, 1009
- Noguchi, M. 1991, *MNRAS*, 251, 360
- Rubin, V. C., Kenney, J. D. P., & Young, J. S. 1997, *AJ*, 113, 1250
- Sanders, D. B., & Mirabel, I. F. 1996, *ARA&A*, 34, 749
- Springel, V., & White, S. D. M. 1998, *MNRAS*, submitted
- Toomre, A., & Toomre, J. 1972, *ApJ*, 178, 623
- Turner, E. L. 1976a, *ApJ*, 208, 20
- Turner, E. L. 1976b, *ApJ*, 208, 304
- Vorontsov-Vel'yaminov, B. A. 1959, *Atlas and Catalog of Interacting Galaxies (Moscow: Sternberg State Astronomical Institute)*

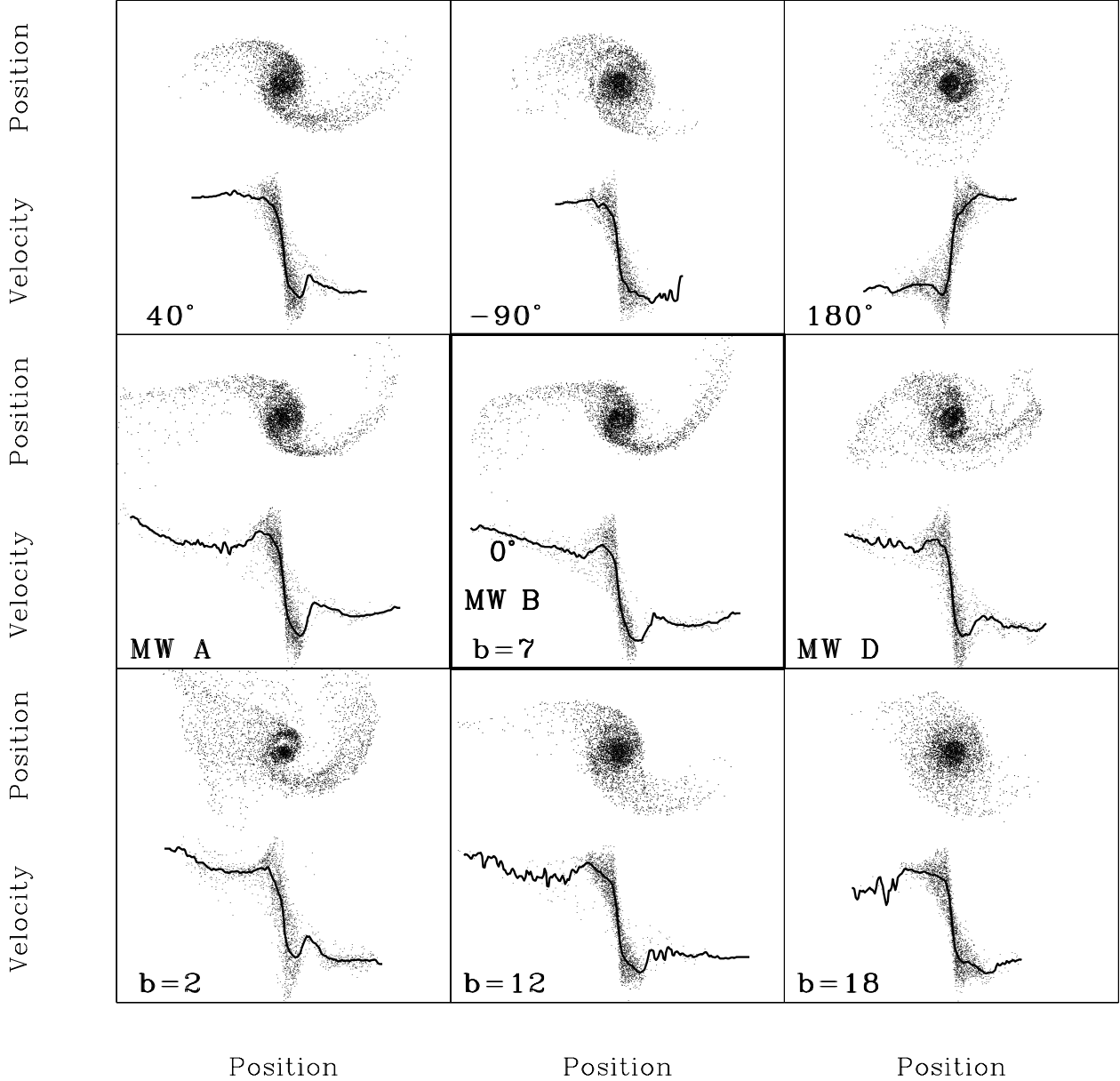


Fig. 1.— Galaxies and rotation curves from the kinematic models. In each case the simulations are two colliding galaxies are of the same Milky Way model; we show only one of the galaxies in each square. The middle box is the fiducial simulation, a “Milky Way B” (MW B), prograde (0° inclination) galaxy with an impact parameter of $b = 7$. The other boxes contain variants on this simulation. The *top* row shows MW B models with impact parameters $b = 7$ and varied orbital inclinations (i); they are: (a) $i = 40^\circ$, with Toomre disk orientation parameter $\omega = 30^\circ$ (b) $i = -90^\circ$, $\omega = 40^\circ$, and (c) $i = 180^\circ$ (retrograde). The *middle* row shows models with impact parameters $b = 7$ and inclinations $i = 0^\circ$ with varied galaxy models; they are (d) MW A (e) MW B and (f) MW D. The *bottom* row shows MW B models with inclinations $i = 0^\circ$ and varied impact parameters; they are: (g) $b=2$, (h) $b=12$ and (i) $b=18$.

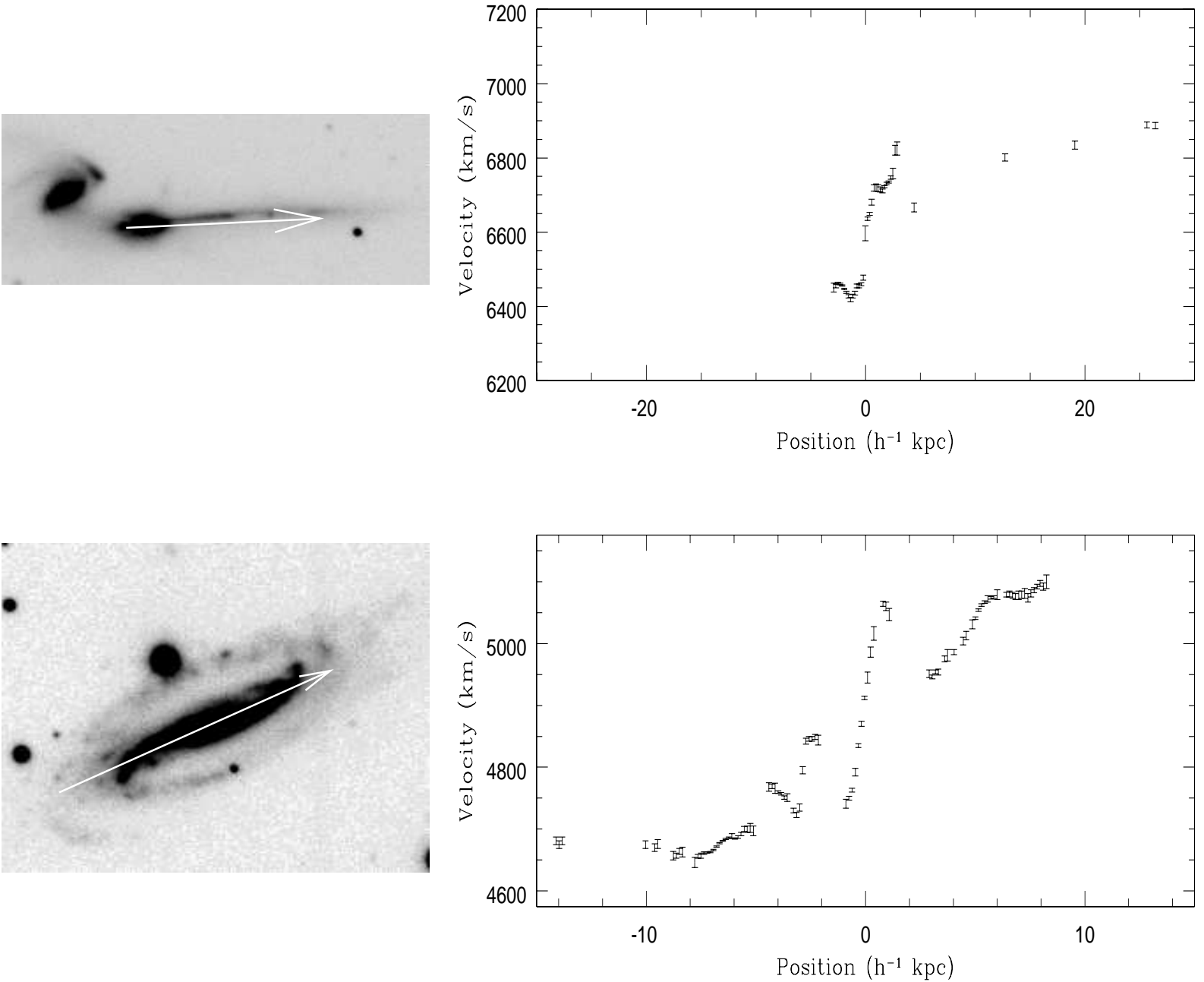


Fig. 2.— B Images and rotation curves for two galaxies in the sample: (a) NGC 4676, “The Mice” and (b) UGC 484, a barred spiral. Arrows show the slit position; they point in the direction of increasing position.